Journal of Applied Polymer Science

Molecular, Rheological, and Thermal Study of Long-chain Branched Polypropylene Obtained by Esterification of Anhydride Grafted Polypropylene

Jorge Guapacha,[1] Marcelo D. Failla,[1,2] Enrique M. Vallés,[1] Lidia M. Quinzani[1]
[1]Planta Piloto de Ingeniería Química (PLAPIQUI), UNS-CONICET—C.C. 717, Bahía Blanca 8000, Argentina
[2]Departamento de Ingeniería, Universidad Nacional del Sur (UNS), Alem 1253, Bahía Blanca 8000, Argentina
Correspondence to: L. M. Quinzani (E-mail: lquinzani@plapiqui.edu.ar)

ABSTRACT: Long-chain branched polypropylene was prepared using reaction in the molten state in the presence of glycerol and a linear polypropylene functionalized with maleic anhydride (PPg). The concentration of glycerol in the melt was varied in the range from 0.1 to 5 wt % to obtain different levels of branching. FTIR spectroscopy results indicate that the OH groups of glycerol react with the anhydrides on the PPg chains giving place to ester groups. The presence of long-chain branches in the molecular structure of PPg was confirmed using multiple-detection size-exclusion chromatography and rheology. These techniques demonstrate that the level of branching increases with glycerol concentration and that the modification of PPg produces materials with a bimodal distribution of polymer species. Moreover, some of the highly modified materials display gel-like behavior. The materials also display thermo-rheological complexity and enhanced activation energy at low frequencies. The crystallization study shows that both the anhydride groups in PPg and the LCBs have opposite nucleating effects. PPg presents the largest activation energy of crystallization and its value decreases with the concentration of glycerol for a given level of crystallization. © 2014 Wiley Periodicals, Inc. J. Appl. Polym. Sci. **2014**, *131*, 40357.

KEYWORDS: polyolefins; structure–property relations; crosslinking

Received 28 November 2013; accepted 30 December 2013
DOI: 10.1002/app.40357

INTRODUCTION

Polypropylene (PP) has become one of the most widely used commercial polyolefins. It is synthesized employing either Ziegler–Natta or metallocene catalysts, which produce highly linear stereospecific polymers. PP possesses many excellent properties, such as low density, high melting temperature, stiffness, good chemical resistance and recyclability. Its main drawback is the low melt strength and poor melt strain hardening that limits the use of PP in certain applications like thermoforming, foaming, blow molding and film molding.[1–3] The melt strength of PP is a function of molecular weight, polydispersity, degree of long-chain branches and entanglement density. Still, the most effective strategy to improve the melt strength of this polymer has been to modify the topology of the linear molecules by introducing long-chain branches (LCB).[4–22] The presence of LCBs strongly inhibits the reptation mechanism for configurational rearrangement of flexible macromolecules, increasing the terminal relaxation time, enhancing the melt strength and improving the strain hardening behavior of the material in extensional flows.[6,8,10–12,15,16,18,21,23]

Several strategies have been then attempted to introduce long chain branches onto PP. By means of *in situ* polymerization, the branches are generated during the polymerization of propylene in the presence of a nonconjugated diene such as *p*-(3-butenyl)-styrene. In this case, the incorporation of the comonomer onto the polymer backbone gives origin to ramification points that, in principle, can be tuned according with the comonomer content.[13,14,18] Simpler approaches, due to its versatility and ease of use by polymer processers, are those that involve post polymerization modifications by irradiation, solid-state grafting, or by reactive extrusion in the melt. In the irradiation approach the branches are produced from the combination reaction of the macro radicals generated by the excitation of the PP molecules with electron beam irradiation or electromagnetic waves. This process is commercial available and the final branching level depends of the processing conditions and the applied dose.[5,6,10,11,16] In the solid-state grafting, the chemical modification of the PP is initiated by radicals generated by peroxide that is followed by the grafting of PP molecules at low temperature.[8] Reactive extrusion involves the chemical attack of PP in the molten state in the presence of peroxide and a polyfunctional

monomer. The peroxide decomposition induces the formation of macroradicals that react with the added monomer promoting the generation of branches and inhibiting the scission of the PP chains.[4,6,7,9,12,15,17,20–22] The reactive extrusion process may also be applied to a functionalized PP, such as maleic anhydride grafted PP (PPg), which is melt blended with just the polyfunctional monomer or oligomer.[19]

Among the previous methods, reactive extrusion is the most suitable from the industrial point of view, and has been chosen in this work to produce long-chain branches in a functionalized commercial PPg. Glycerol has been selected as the crosslinking agent due to its availability and low cost, and because is a harmless material that reacts easily with anhydride groups. The reaction between the anhydride groups of PPg and the OH groups of the multifunctional agent was performed in the molten state. To verify the extent of the esterification reaction and the amount of long chain branching induced on the polymer chains, the original and modified polymers were characterized using infrared spectroscopy (FTIR) and size exclusion chromatography at high temperature (SEC). The materials were also characterized using small amplitude oscillatory shear flow and differential scanning calorimetry (DSC).

EXPERIMENTAL

Materials

The polymer used in this work is a PPg from Uniroyal Chemical (Polybond 3200, $M_w = 120{,}000$ g mol^{-1} and $M_w/M_n = 2.6$). The infrared spectra of the commercial PPg shows the presence of acid groups in the molecules than can be associated to the hydrolysis of the some of the anhydride groups. Therefore, the polymer was thermally treated at 130°C under vacuum during 8 h to allow the recuperation of the anhydride groups. The amount of anhydride groups (AG) in the treated PPg was determined by infrared spectroscopy and estimated in 0.74 wt %, which indicates the existence of approximately four AGs in an average PPg molecule. The material used in this work was previously purified by dissolving the PPg in xylene and then precipitating it with methyl-ethyl-ketone.[24] The crosslinking agent employed to induce the formation of long branches was bidistilled glycerol (99.5% pure) from Anedra Research AG S.A. that was used as purchased.

Modification of PPg

The reaction between PPg and glycerol was performed in a Brabender Plastograph® mixer at 190°C and 40 rpm for 15 min. Then, the unreacted glycerol was removed from the modified polymer by dissolving the materials in xylene at 120°C under constant stirring and in a nitrogen atmosphere. The polymer was then precipitated using cold methyl-ethyl-ketone, and dried at 80°C for 48 h under vacuum.

The modified PPgs are identified as PPgG# where # is representative of the weight percentage of glycerol used in the modification, ranging from 0.1 to 5 wt % (see Table I).

Characterization

The amount of anhydride groups that reacted with the glycerol in each case was determined by FTIR spectroscopy using a Nexus spectrophotometer from Nicolet. The spectra were obtained on ~100-μm-thick films using a resolution of 4 cm^{-1}.

Table I. Molecular Parameters of PPg and the Modify Polymers

	Weight % glycerol added	Mass recovery (%)	M_n (kg mol^{-1})	M_w (kg mol^{-1})	M_w/M_n
PPg	0	100	48.6	132	2.7
PPgG01	0.11	97	52.3	161	3.1
PPgG02	0.21	98	69.8	241	3.4
PPgG03	0.31	99	60.5	403	6.7
PPgG06	0.60	92	69.8	378	5.4
PPgG08	0.79	92	81.0	424	5.2
PPgG09	0.91	88	108	522	4.8
PPgG1	1	85	265	832	3.1
PPgG5	5	76	364	1010	2.8

The weight average molecular weight (M_w) and the number average molecular weight (M_n) of PPg and all the synthesized materials were estimated by SEC at 135°C using a Viscotek 350 system from Malvern provided with three detectors: light scattering (LS), refraction index and on-line viscometer. The chromatograph was equipped with a set of PLgel 10 µm Mixed-B LS columns (Polymer Labs). The 1,2,4-trichlorobenzene containing 0.1 wt % of butyl hydroxyl toluene was used as solvent. The system was calibrated with standards of polystyrene (Viscotek) of 98,000 and 228,200 g mol^{-1}.

The dynamic moduli of the polymers were determined using small-amplitude oscillatory shear flow in an AR-G2 rheometer from TA Instruments equipped with 25 mm diameter parallel plates. The rheometer was operated under stress-controlled mode. The samples used in the rheological tests were prepared by compression molding at 180°C. The linear viscoelastic behavior of the different polymers was studied at 180°C, at frequencies between 0.01 and 200 s^{-1}, applying a constant shear stress of 10 Pa. Under these conditions the rheological measurements were well under linear viscoelastic range.

Thermal analysis was carried out on a Pyris 1 calorimeter from Perkin Elmer. The samples were heated from 30 to 180°C under nitrogen atmosphere and held at this temperature for 3 min in order to erase their thermal history. Then, they were cooled to 30°C and heated again up to 180°C. Heating and cooling rates of 10°C min^{-1} were used in all cases. The crystallinity of PPg and modified polymers was determined from the last scan according to:

$$X_c = \frac{\Delta H_c}{\Delta H_f^0} \times 100 \quad (1)$$

where ΔH_c is the specific crystallization enthalpy of the samples and ΔH_f^0 is the melting enthalpy of an hypothetical 100% crystalline PP ($\Delta H_f^0 = 209$ Jg^{-1}).[25]

All runs, performed using the techniques described above, were repeated using at least two different samples of each material to ensure reproducibility.

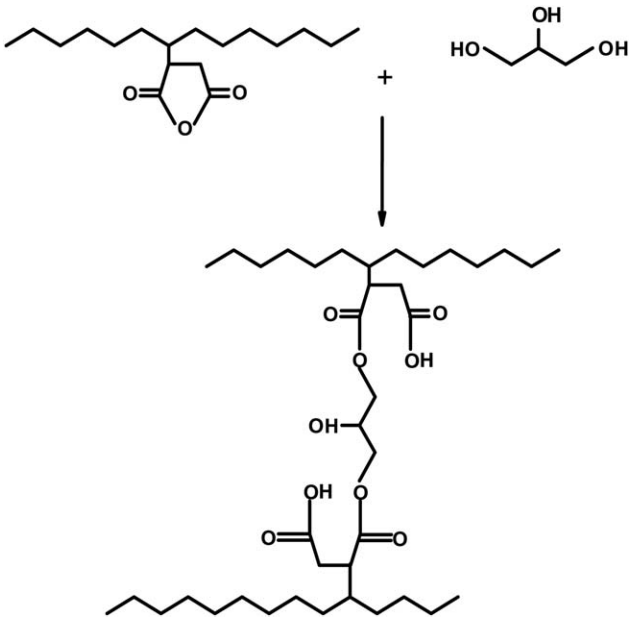

Figure 1. Simplified mechanism for the formation of PPgG molecules.

RESULTS AND DISCUSSION

Molecular Characterization

The modification of PPg with glycerol produces ester groups due to the reaction of the grafted anhydrides on the PPg with the hydroxyls groups of the glycerol. Because each molecule of glycerol has three hydroxyl groups, it can react with more than one anhydride inducing chain linking between macromolecules. The scheme in Figure 1 illustrates one possible reaction between one glycerol and two PPg molecules. The original position of the anhydrides along the backbone of the PPg molecules determines the final structure of the PPgGs. Linear, branched and complex H-shaped or tree-shaped topologies, among others structures, can be expected from this reaction.

FTIR spectroscopy can be used to analyze the chemical changes that occur after the reaction. Figure 2 shows two regions of the infrared spectra of the original PPg and of the obtained PPgGs. One of these regions includes the absorbance bands associated to carbonyl groups,[26] and the other the reference band of 2720 cm^{-1}. The absorbance of this last band corresponds to the methyne groups (CH) of the PP backbone[26] and it was used to normalize all the spectra. Bands at 1792 and 1860 cm^{-1} that appear in the PPg and PPgGs spectra correspond to the symmetrical and asymmetrical C═O stretching of anhydride. Additionally, the PPgGs present bands at 1715 and 1735 cm^{-1} that can be assigned to the stretching of carbonyls of acid and ester groups respectively. The results clearly show that the absorbance corresponding to these groups rises when the dose of glycerol used in the process increases.

To quantify the amount of anhydrides in each material, the absorbance of the band at 1792 cm^{-1} (A_{1792}) relative to the absorbance at 2720 cm^{-1} (A_{2720}) is compared with the calibration curve:

$$\frac{A_{1792}}{A_{2720}} = 1.298\%\ AG \quad (2)$$

This curve was obtained measuring the absorbances of physical mixtures of succinic anhydride with PP in concentrations ranging from 0.2 to 3 wt %.[27]

Figure 3 displays the concentration of AG in each polymer estimated with eq. (2) as a function of the concentration of glycerol. The value calculated for PPg (also determined with this equation) is located at 0% of glycerol. Figure 3 also includes the value of the absorbance corresponding to the carbonyl groups of the generated esters, located at 1735 cm^{-1} (A_{1735}) relative to the reference band, A_{2720}. As expected, the concentration of anhydride groups decreases as the concentration of glycerol raises and the A_{1735}/A_{2720} ratio grows. This is because the amount of anhydrides that react to give ester groups increases. Both, the A_{1735}/A_{2720} ratio and the concentration of AG in the modified polymers have a linear dependency with the concentration of glycerol up to ~0.3 wt %. At larger concentrations, both the amount of AGs and the ratio of absorbance change at a very low rate. The concentration of AG decay from ~0.4 to 0.27 wt % and the ratio A_{1735}/A_{2720} from 0.4 to 0.5 when the concentration of glycerol goes from 0.3 to 5 wt % (the PPgG5 results are not included in Figure 3 for clarity reasons). This means that approximately half of the original AGs in PPg does not react for concentrations of glycerol above 0.6 wt %. A lack of accessibility of the glycerol molecules to the AGs still present in the modified PPg molecules and the phase separation of glycerol, may be the causes of this behavior.

The PPg and the modified polymers were characterized by SEC coupled with triple detectors to determine the molecular weight distributions, the corresponding average molecular weights and the topological structure of the molecular chains. While

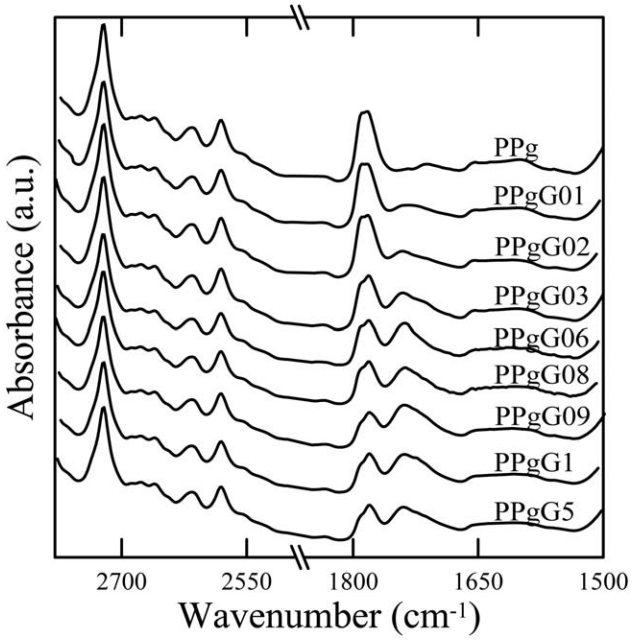

Figure 2. FTIR spectra of PPg and modified materials. The numbers next to the curves correspond to the weight percent of glycerol used.

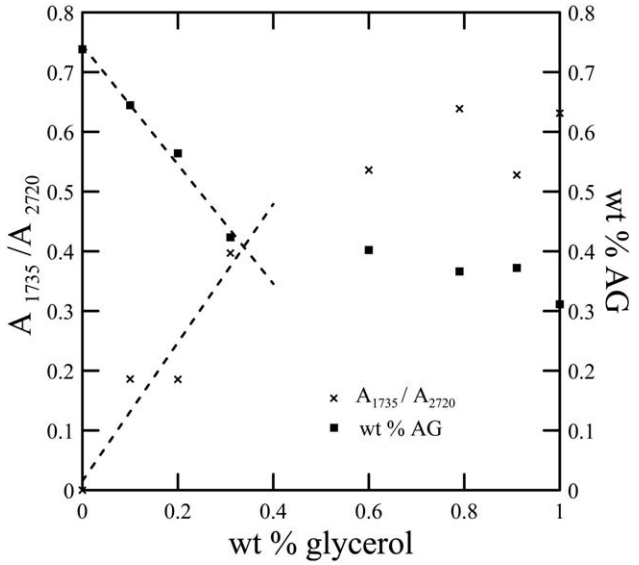

Figure 3. Ratio of absorbances A_{1735}/A_{2720} (left) and concentration of AG (right) of the different polymers as a function of the concentration of glycerol.

performing the SEC experiments it was observed that for some of the PPgGs a noticeable amount of material was retained by the filtration system of the equipment. This problem was present on the polymers reacted with concentrations of glycerol above 0.3 wt %. It was also verified that the amount of material hold on by the filters increased with the concentration of glycerol employed to modify the PPg. The percentage of recovered mass for the different polymers was calculated using a *dn/dc* of -0.098 mL g^{-1} which was estimated for complete mass recovery of PPg. The computed *dn/dc* is close to the value of −0.105 mL g^{-1} reported for iPP in 1,2,4-trichlorobenzene.[28] The percentage of mass recovery estimated in this way for each of the polymers is reported in Table I. It may be mentioned that a 5% change in the value of *dn/dc* produces a change of 6% in the calculated recovered mass.

The increase in mass loss with glycerol concentration indicates the presence of a gel fraction, at least above 3 wt %. To verify this observation, samples of PPgG1 and PPgG5 were dissolved in xylene at 130°C, kept at these conditions during 20 h, and then filtrated to separate the soluble material. The retained material was dried under vacuum and the gel fraction of the polymer was determined by the ratio of the dried mass retained to the initial mass. Fractions between and 10 and 20 wt % were measured, in concordance with the results from SEC.

The normalized chromatograms from the LS detector corresponding to PPg and the modified materials are shown in Figure 4. Light scattering is a technique very sensitive to the presence of high molecular weight macromolecules. The data shown in Figure 4, which were obtained from the 90° angle detector, are very similar to those register from the 7° angle detector (not shown). The two sets of data in Figure 4 correspond to the materials with no evidence of gel fraction (main figure) and those with a detectable gel fraction (inset). The chromatogram of PPgG06 is included in both sets for comparison. PPg exhibits a typical chromatogram of a polymer with a Gaussian distribution of molecular weights while the rest of the polymers display bimodal distributions. The modified materials present one peak corresponding to the remaining population of unmodified PPg, and a second peak placed at smaller retention volumes that correspond to new macromolecules of larger molecular weight. As expected, for glycerol concentrations up to 0.6 wt %, the peak of the PPg population decreases gradually as the concentration of glycerol employed to modify the polymer increases, while the other peak gets larger. The soluble part of the polymers obtained with more than 0.6 wt % of glycerol keeps this tendency up to 0.9 wt %, although with a smaller rate of change. For even larger concentrations (1 and 5 wt %) most of the high molecular weight fraction of the modified materials is retained by the filters. For this reason, the sol fractions analyzed in the chromatogram display similar concentrations of the high and low molecular weight fractions.

Figure 5 displays the molecular weight distributions of all polymers. As it may be observed, PPgG01 already shows a broader molecular weight distribution than PPg with a small tail of high molecular weight material. These effects get more noticeable as the concentration of glycerol augments. Up to 0.6 wt % glycerol, the chromatograms display a gradual increase of the high molecular weight tail with a shift of the whole distribution of molecular weights to larger values. As already mentioned in the discussion of Figure 4, the data corresponding to the use of more than 0.6 wt % of glycerol may be associated only to the molecular weight distributions of the soluble fractions of these polymers. Nonetheless, the chromatograms display a further and gradual shift to larger molecular weights with a decreasing tail of low molecular weight.

Table I lists the average molecular weights calculated from the molecular weight distributions displayed on Figure 5 corresponding to the soluble fraction of the polymers. The number

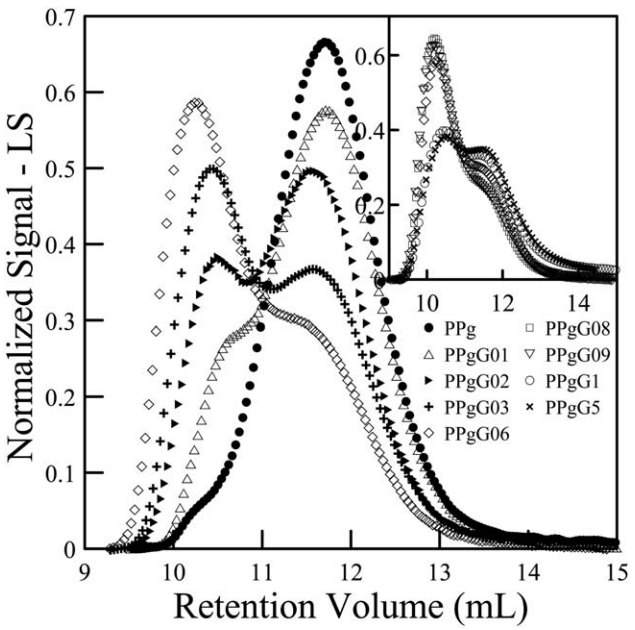

Figure 4. Chromatograms of PPg and the modified polymers (normalized with the area) obtained by SEC using the light scattering detector.

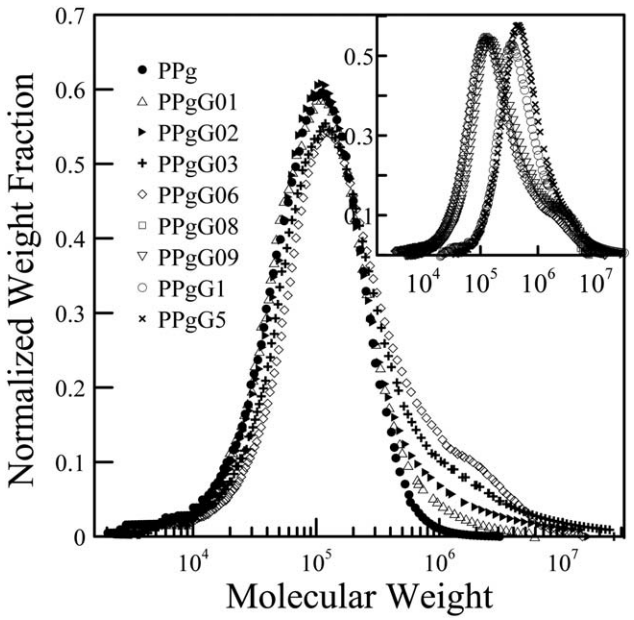

Figure 5. Molecular weight distributions of all materials, normalized with the curve areas.

and weight average molecular weights increase gradually with the concentration of glycerol used in the modification process, even for the materials prepared with more than 0.6 wt % glycerol. The ratio M_w/M_n, however, increases up to PPgG03 and then decreases gradually as the amount of retained mass increases. This behavior of M_w/M_n suggests that there is a critical concentration between 0.3 and 0.6 wt % above which, at the same time that the low molecular weight fraction reduces as the concentration of glycerol augments, the high molecular weight fraction also reduces because a considerable part of it is being retained by the equipment filters.

The intrinsic viscosity data obtained from SEC with multiple detectors can be used to evaluate the type of structure of the generated high molecular weight fractions. Figure 6 presents the data obtained for PPg and the modified materials PPgG01, PPgG02 and PPgG03. The straight line that appears in this figure corresponds to the prediction of the Mark-Houwink relation, that is $[\eta] = KM^a$, where $[\eta]$ is the intrinsic viscosity, M the molecular weight, and K and a are the Mark–Houwink constants. This relation applies to polymers with molecules of linear structure, like PPg. The fitting of the PPg data to this model results in $a = 0.69$ and $K = 1.74 \times 10^{-4}$. These values are very close to those reported in the literature for linear PP.[18,29] As the molecular structure of a polymer becomes more complex, the radius of gyration for a given molecular weight gets smaller. Consequently, the intrinsic viscosity associated to that molecular weight also gets smaller and separates from the Mark–Houwink relation. The intrinsic viscosity data of the modified materials presented in Figure 6 display this behavior, validating the conclusion that, as the concentration of glycerol increases, the degree of branching and the complexity of the generated branched structures increases. Furthermore, for each of these polymers the intrinsic viscosity data corresponding to high molecular weights get further apart from the linear behavior as the molecular weight increases.[18,21] It also may be observed that the data corresponding to the low molecular weight fractions align on the straight line indicating linear structures. The results for all the rest of the polymers deviate from the Mark–Houwink prediction in the whole range of molecular weights and are not included in Figure 6.

It is well known that the behavior of branched polymers in solution is related to the size of their molecules through the mean square gyration radius, the intrinsic viscosity and the hydrodynamics radius.[30,31] According to the model of Zimm and Stockmayer, combined with the methodology of Lecachaux,[32] the ratio between the mean square radius of gyration of the branched molecules and that of the linear material, $g = \langle S^2_0 \rangle_b / \langle S^2_0 \rangle_l$, is related with the ratio of the intrinsic viscosity of these two type of polymers, g':

$$g^{\varepsilon} = g' = \frac{[\eta_b]}{[\eta_l]} \tag{3}$$

In this equation, ε is a parameter whose value depends on the type of branching and solvent–polymer interaction. It has been suggested that ε has a value of 1/2 for star polymers, 3/2 for combs with large backbones and short branches and 0.7 for a multiarm stars.[33–35] For random branching, a value of 0.75 is often used,[7] and the average number of branches per macromolecule, m, is calculated from this ratio using the equation:

$$g = \frac{6}{m}\left[\frac{1}{2}\left(\frac{2+m}{m}\right)^{0.5} \ln\left(\frac{(2+m)^{0.5}+m^{0.5}}{(2+m)^{0.5}-m^{0.5}}\right) - 1\right] \tag{4}$$

Finally, the number of branches per 1000 monomer units, N_{LCB}, can be estimated from:

$$N_{LCB} = 1000 \times M_M \times \frac{m}{M} \tag{5}$$

where M_M is the molar mass of the monomer and M is the molar mass of the branched polymer.

Figure 7 presents the data of N_{LCB} estimated for the polymers in Figure 6 using the equations above. Values of $\varepsilon = 0.75$ and $M_M = 42$ g mol^{-1} where considered in these calculations. Even though eq. (4) may not be strictly applicable to the modified

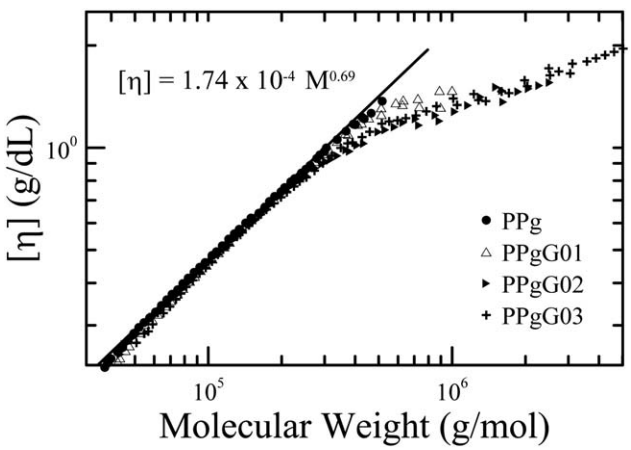

Figure 6. Intrinsic viscosity as a function of molecular weight of PPg and the modified polymers PPgG01, PPgG02, and PPgG03.

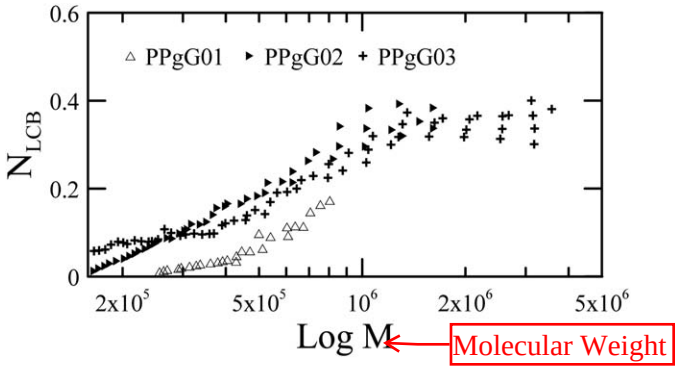

Figure 7. Estimated numbers of branches per 1000 monomer units as a function of molecular weight for PPgG01, PPgG02, and PPgG03.

polymers, we use it as a way of comparing the changes in their molecular structures. The data in the figure support previous conclusions that as the concentration of glycerol used in the modification increases, the population of large molecular weight that is generated has a complex structure with increasing numbers of branches per molecule. The results in Figure 7 suggest that the larger macromolecules that are generated during the modification process present up to two branches every 10^4 carbons, which is the average number of carbons expected in an average PPg molecule. Other authors have estimated similar values for synthesized branched PPs using different methods.[6,7,12,14,17,18]

Linear Viscoelastic Characterization

The linear viscoelastic behavior of polymers is very sensitive to structural changes in the topology of macromolecules. Therefore, the comparison of dynamic moduli has become one of the most reliable techniques to verify the existence of long branches in polymer chains.[9,13–15,17,18,20–23,35,36] As the molecular topology of a polymer becomes more complex and/or its molecular weight increases, the relaxation times associated to those structures increase, which affects mainly the properties obtained at low deformation rates.

Figure 8 displays the elastic (G') and the viscous (G'') moduli of all analyzed polymers. PPg has the typical rheological behavior of a linear polymer, where G' and G'' exhibit frequency dependence close to ω^2 and ω at low frequencies, respectively. This is the terminal region, where the longer relaxation times contribute to the viscoelastic behavior. As the concentration of glycerol used in the modification of PPg increases, the dynamic properties become significantly enhanced in comparison with those of the linear polymer, being the effect more noticeable in G' and mainly at low frequencies. At high frequencies, where the viscoelastic response is mainly due to the dynamic of short segments of the macromolecules, the dynamic moduli of all materials converge to similar values. At low frequencies, however, the enhancement of both moduli and the reduction of the phase angle ($\tan\delta = G''/G'$) with the augment of the concentration of glycerol is remarkable. This behavior implies the presence of a long relaxation time mode and agrees with the increasing complexity of the modified molecules, as already discussed. The branched macromolecules present larger relaxation times as the concentration of branches increases. Moreover, the highly modified materials display gel-like behavior.

To further study the effect of LCBs in the rheological response of the polymers, the thermorheological response of some of the materials was analyzed. It is known that linear polymers obey the time-temperature superposition principle and are thermorheologically simple materials. However, long-branched polymers usually do not obey the superposition principle because of the constraints imposed by branching points on chain relaxation, becoming thermorheologically complex. Furthermore, the flow activation energy corresponding to low frequency data increases with the addition of LCBs.[3,6,8,14,18,36,37]

Figure 9 displays the master curves of the phase angle of PPg obtained from data measured at temperatures between 173 and

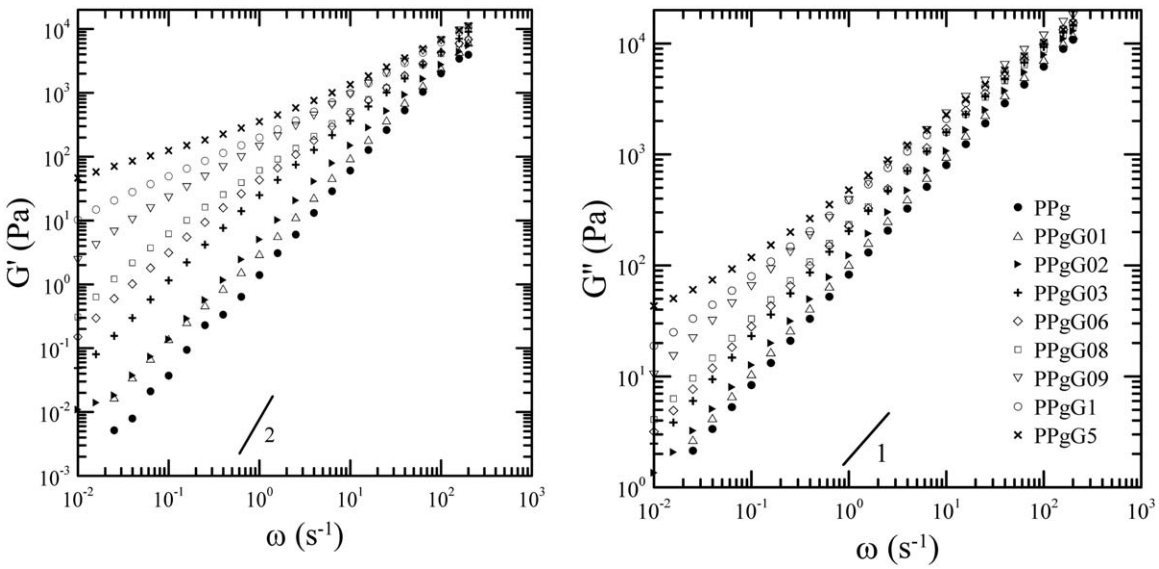

Figure 8. Elastic (left) and viscous (right) moduli of all polymers as a function of frequency at 180°C.

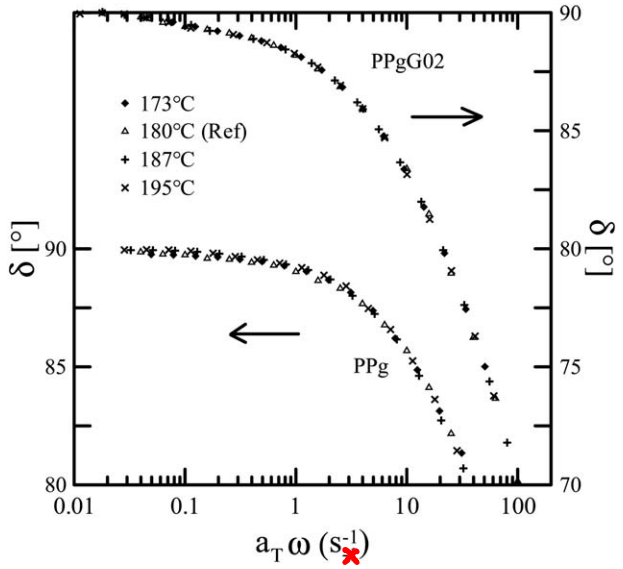

Figure 9. Master curves of the phase angle of PPg and PPgG02 at $T_0 = 180°C$.

195°C. Each curve of data was shifted along the frequency axis until superposition with those at 180°C. As it can be appreciated, PPg displays thermorheologically simple behavior in this range of temperatures. The fitting of the calculated time-temperature shift factors (a_T) to the Arrhenius model, gives an activation energy (E_a) of 44.7 kJ mol^{-1}, which is within the range of values reported in the literature for lineal PP.[2,8,13,18] The time-temperature superposition principle failed in the case of PPgG02. If the curves are superimposed at low values of phase angles (high frequencies), they separate at higher δ. Therefore, a unique shift factor does not exist.

The master curve of δ of PPgG02 that appears in Figure 9 was obtained by shifting each data horizontally up to superposition

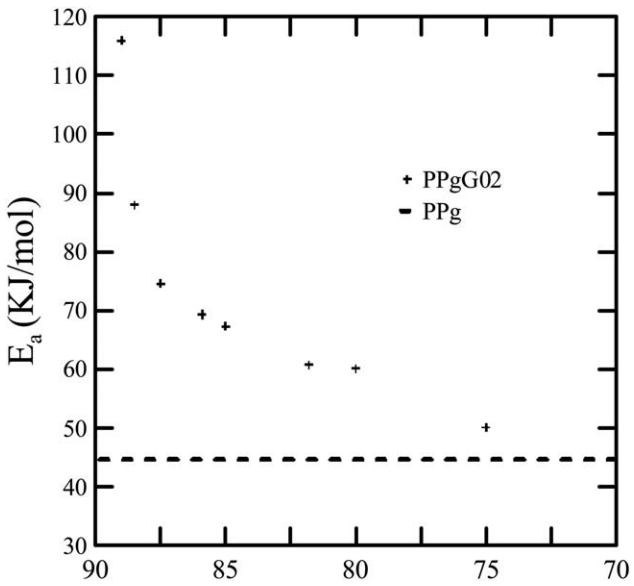

Figure 10. Activation energy spectra for PPgG02 referenced to 180°C.

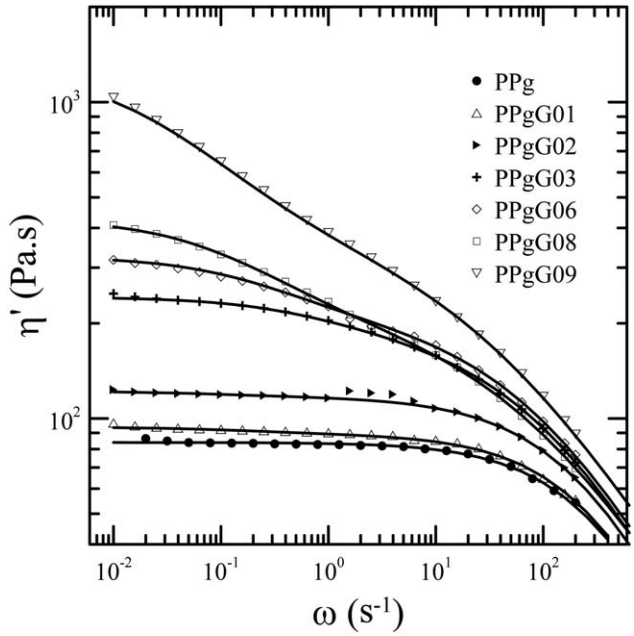

Figure 11. Dynamic viscosity as a function of frequency at 180°C, and predictions of the two-mode Cross model [eq. (6)].

with the curve at 180°C, that is, different shift factors were used for each data at each temperature.[14,36,37] The a_T factors used to shift the data at given values of the phase angle were then plotted as a function of $1/T$ and activation energies were calculated using the Arrhenius model. The activation energies calculated in this way are displayed in Figure 10. As it may be appreciated, at high frequencies (low δ), E_a has a value similar to that of PPg and it rapidly increases toward the terminal region ($\delta \rightarrow 90°$). The failure of the time-temperature superposition is typical of a thermorheologically complex material, and the large increase in the value of E_a associated to the terminal relaxation time, is another evidence of the existence of molecules with branched topologies.

Figure 11 shows the dynamic viscosity (η') of all samples at 180°C. This way of presenting the dynamic data emphasizes the increasing complexity of the molecular structure. The typical plateau of constant viscosity at low frequencies (η_0) displayed by PPg gradually shifts towards lower frequencies and higher values as the concentration of glycerol increases. Furthermore, as the concentration of LCBs increases, the shear-thinning region becomes more appreciable, beginning at gradually lower frequencies. This behavior is typical of topological structures that get gradually more complex.[6,14,15,17,18,20–22] An additionally interesting behavior can be also observed when the dynamic data are presented in this way. As the concentration of glycerol increases, an inflexion point appears at intermediate frequencies that become increasingly noticeable. A similar behavior was obtained by Nam et al.[15] in the data of $\eta^*(\omega)$ of PPs modified by reactive extrusion. The rheological response of the modified materials looks like that of a blend of two populations of molecular structures with distinctive relaxation times. At the light of this response, the η' data were fitted to a two-mode Cross model.[3]

Table II. Parameters of the Two-mode Cross Model used in the Fitting of the Data of Figure 12

	PPg	PPgG01	PPgG02	PPgG03	PPgG06	PPgG08	PPgG09
η_H (Pa s^{-1})	84	89	117	184	205	200	350
λ_H (s)	0.0026	0.0028	0.0038	0.01	0.012	0.016	0.04
n_H	~0.8	0.8	0.75	0.64	0.62	0.56	0.54
η_L (Pa s^{-1})	-	5	5	58	120	230	930
λ_L (s)	-	~1	~1	1.1	3.5	6	28
n_L	-	(0.8)	(0.8)	0.8	0.8	0.75	0.7
η_H/η_L	-	18	23	3.2	1.7	0.87	0.38
λ_L/λ_H	-	-	-	110	290	375	700

$$\eta'(\omega) = \frac{\eta_H}{1+(\lambda_H\omega)^{n_H}} + \frac{\eta_L}{1+(\lambda_L\omega)^{n_L}} \quad (6)$$

where the subscripts H and L stand for high and low frequencies respectively, and η_i, λ_i, and n_i are the corresponding zero-shear viscosity, characteristic relaxation time and shear-thinning index of each mode, respectively. PPgG1 and PPgG5 are not included in Figure 11 because they present yield stress and the viscosity data cannot be modeled with eq. (6). The computed parameters of the other polymers are listed in Table II, and the dynamic viscosities predicted with eq. (6) are included in Figure 11. It can be observed that the data of PPg are well modeled by the Cross model using a single relaxation time, while the viscosity data of all the other materials are described by two relaxation modes. The mode corresponding to the smaller relaxation time describes the high frequency data and can be associated to the population of PPg and/or simpler molecules. The second mode, which corresponds to the higher relaxation time, affects the low frequency region and can be associated to the generated high molecular weight material. It may be observed that, although the relaxation time associated to the simpler material, λ_H, increases gradually with the augment of glycerol concentration, the relaxation time that corresponds to the new high molecular weight material, λ_L, is at least two orders of magnitude larger and increases more rapidly. Moreover, as the concentration of glycerol increases, the first mode gradually losses importance when compared to the new one (η_H/η_L decreases).

Using molecular dynamics, Tian et al.[17] were able to estimate the ratio of the relaxation time of long-branched molecules of PP to the relaxation time of the linear material. They obtained values that range from 6.5 to 80 as the concentration of the crosslinking agent, pentaerythritol triacrylate, increases. They also estimated the level of LCBs in the range of 0.025 to 0.38/10^4 carbons. In the present work, the synthesized materials present larger ratios of relaxation time, which may be associated to the larger levels of long branches.

Thermal Analysis

The change in the molecular structure of a polymer may produce changes in its thermal behavior. In this section we analyze the melting and crystallization process of the synthesized materials by differential scanning calorimetry as described in Experimental section. Figure 12 displays the thermograms of the

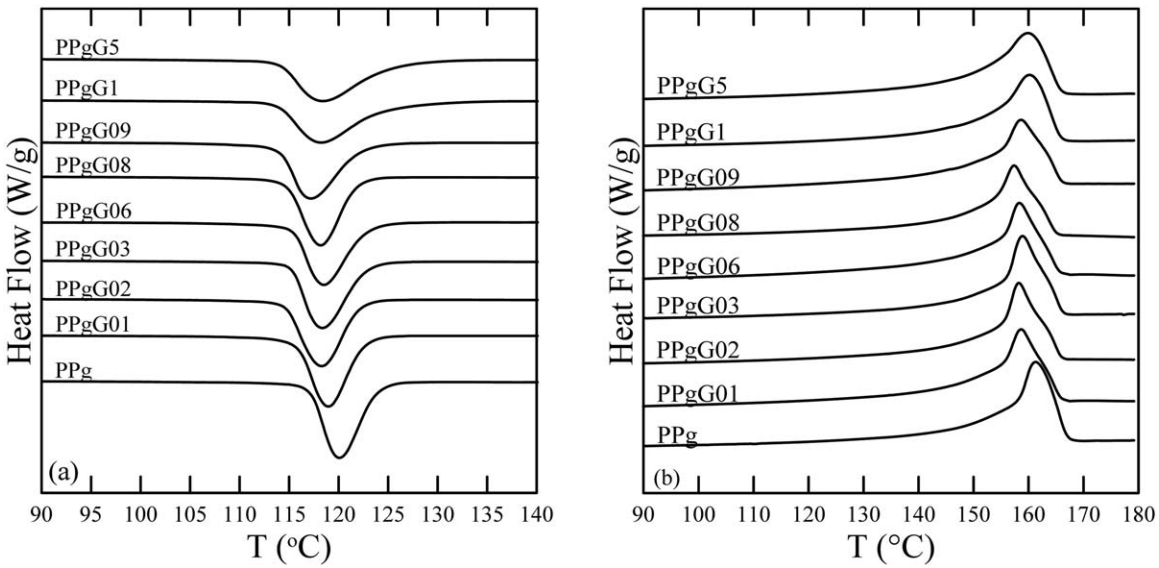

Figure 12. Thermograms of PPg and the modified polymers during crystallization (a) and melting (b).

Table III. Thermal Properties of PPg and the Modified Polymers

	PPg	PPgG01	PPgG02	PPgG03	PPgG06	PPgG08	PPgG09	PPgG1	PPgG5
T_m (°C)	161	159	158	159	158	157	159	160	160
ΔH_m (J g^{-1})	105	104	103	102	106	104	101	101	101
T_c (°C)	120	119	118	118	118	118	117	118	118
ΔH_c (J g^{-1})	101	96.0	95.9	97.1	93.1	93.2	93.1	95.4	94.7
$T_{c\ onset}$ (°C)	125	124	123	124	125	123	125	132	131
$t_{1/2}$ (min)	0.50	0.48	0.48	0.55	0.58	0.44	0.71	1.26	1.21

different materials obtained using 10°C min^{-1} cooling and heating rates. Table III lists the values of the melting (T_m) and crystallization (T_c) temperatures obtained from the maxima of the peaks of the curves in Figure 12. Also listed in Table III are the onset temperature of crystallization (T_{conset}) and the enthalpy of melting (ΔH_m) and crystallization (ΔH_c), which were calculated from the area of the peaks. T_{conset} was computed as the temperature at which the crystallized material is 1% of the total crystallizable material.

The melting process of all polymers is very similar, with T_m and ΔH_m of the modified materials slightly lower than those of PPg. This is in agreement with most of the works in the literature that deal with long-chain branched PPs.[15,16,20,22] The results suggest that the presence of branches in the molecules somewhat reduces the size and amount of the crystal domains.

Regarding the crystallization process, it seems to be more affected by the molecular structure than the melting process. The temperature and enthalpy of crystallization of the modified polymers reduce in ~2°C and 6 Jg^{-1}, respectively, with respect to those of PPg. Furthermore, no noticeable tendency can be appreciated among the data of the PPgG materials. Additionally,

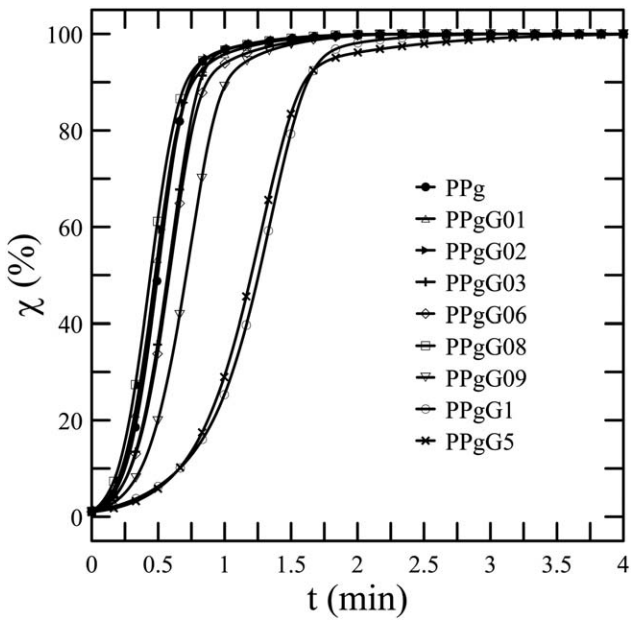

Figure 13. Crystallization enthalpy ratio as a function of time obtained from the data of Figure 12(a).

no change can be appreciated in the value of $T_{c\ onset}$ except in PPgG1 and PPgG5. Most of the works in the literature that analyze the thermal behavior of long branched PPs have found that T_c increases with respect to lineal PP and augments gradually with the degree of LCBs.[9,15,16,20,22,38] These authors associate the observed behavior with the nucleating effect of the LCBs. In the case of a maleic anhydride graphed PP, the AGs act as nucleating agents, producing an increment in T_c (7–10°C) with respect to an equivalent linear PP.[39] The loss of anhydride groups and the generation of LCBs in the PPgGs with respect to the initial PPg may then have two opposite effects on the nucleation. The former cause should produce a reduction in T_c while the last factor may increment this temperature. Although the change in molecular weight is another factor that should be considered, the factors analyzed justify the small reduction in the crystallization temperature observed in this work.

The evolution of the enthalpy of crystallization with time was calculated from Figure 12(a), by the accumulative integration of the curve. These data, divided by the total crystallization enthalpy, ΔH_c, defines the crystallization enthalpy ratio, χ, displayed in Figure 13. The time, t, in this figure was calculated as:

$$t = \frac{T_{c\ onset} - T}{\Phi} \tag{7}$$

where T is the temperature and Φ is the cooling rate (10°C min^{-1} in this case). All curves have the typical S-shape corresponding to a nucleation stage followed by crystal growth. PgG09, PPgG1, and PPgG5 are the materials that present wider range of crystallization temperature and, consequently, slower crystallization rate. From these curves, the crystallization half-time, $t_{1/2}$, defined as the time when the material reaches 50% of its crystallization, can be calculated. The values of $t_{1/2}$ are listed in Table III. The influence of LCB on $t_{1/2}$ is insignificant for glycerol concentrations up to approximately 0.9, being the value of $t_{1/2}$ of PPgG1 and PPgG5 more than double the one of PPg. The augment in the molecular weight and the increase in molecular complexity hinder the crystallization process and justify the increase in $t_{1/2}$.

The analysis of the kinetics of crystallization was completed applying different cooling rates to PPg and two chosen materials, one with low degree of modification (PPgG03) and one of highly modified polymer (PPgG5). Four cooling rates were used: 2.5, 5, 10, and 20°C min^{-1}. The corresponding thermograms are displayed in Figure 14 and the measured properties and calculated parameters are listed in Table IV. As expected, as

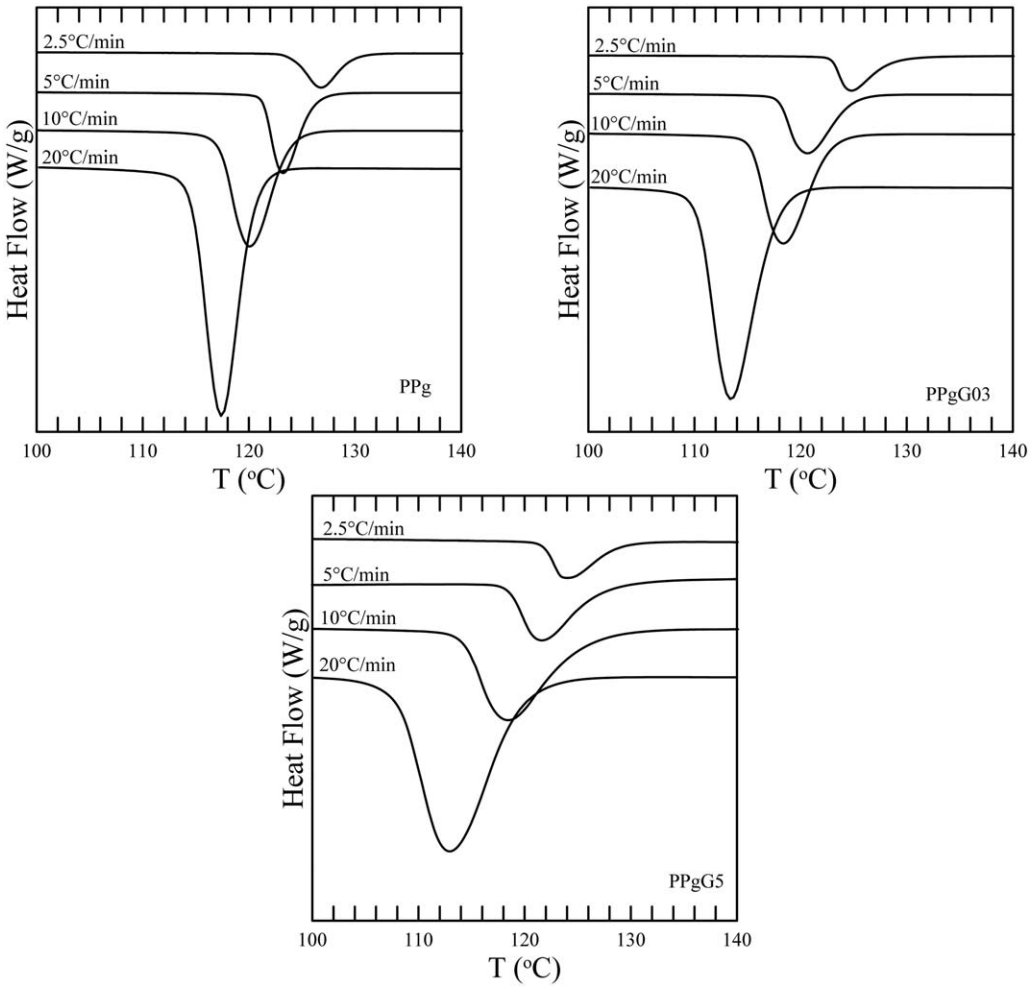

Figure 14. Crystallization thermograms obtained using different cooling rates for PPg, PPgG03 and PPgG5.

the cooling rate increases, the crystallization temperature and the enthalpy of crystallization decrease. A drop of ~10°C can be appreciated between the values of T_c measured at the rates of 2.5 and 20°C min^{-1} for the three compared materials, while a reduction the ~8 Jg^{-1} is observed in the values of ΔH_c. Furthermore, for a given cooling rate, the width of the crystallization range increases as the degree of branching raises. At each cooling rate, the behavior is equivalent to the one observed at 10° min^{-1} and already discussed above.

Table IV. Thermal Properties for PPg, PPgG03, and PPgG5 at Different Cooling Rates

Sample	ϕ (°C min^{-1})	T_c (°C)	$T_{c\ onset}$ (°C)	$t_{1/2}$ (min)	ΔH_c (J g^{-1})
PPg	2.5	127	132	2.0	103
	5	123	128	0.8	99.6
	10	120	125	0.5	101
	20	117	122	0.2	95.1
PPgG03	2.5	125	134	3.3	101
	5	121	126	1.1	95.3
	10	118	124	0.6	97.1
	20	113	119	0.3	95.3
PPgG5	2.5	124	132	3.1	100
	5	122	132	2.0	94.2
	10	119	131	1.2	94.7
	20	113	124	0.5	91.9

A parameter that may be calculated from the crystallization curves is the activation energy of crystallization, ΔE_χ. Several methods have been proposed in the literature for estimating thermal activation energies.[38,40] In particular, the approach suggested by Vyazovkin[41] has been successfully applied in the determination of ΔE_χ.[40] According to this technique

$$Ln\left(\frac{d\chi}{dt}\right)_\chi = Cte - \frac{\Delta E_\chi}{RT_\chi} \quad (8)$$

where $(d\chi/dt)_\chi$ and T_χ are the rate of crystallization and the temperature at a given level of crystallization χ, respectively. The activation energy of crystallization can be obtained from the slope of the plot of $\ln(d\chi/dt)_\chi$ as a function of $1/T_\chi$. Figure 15 shows the values of ΔE_χ calculated for the three polymers of Figure 14 as a function of χ. As expected, the activation energy of all materials is negative. PPg presents the largest $-\Delta E_\chi$. The lineal decrease of this value with χ at low values of crystallization enthalpy ratio

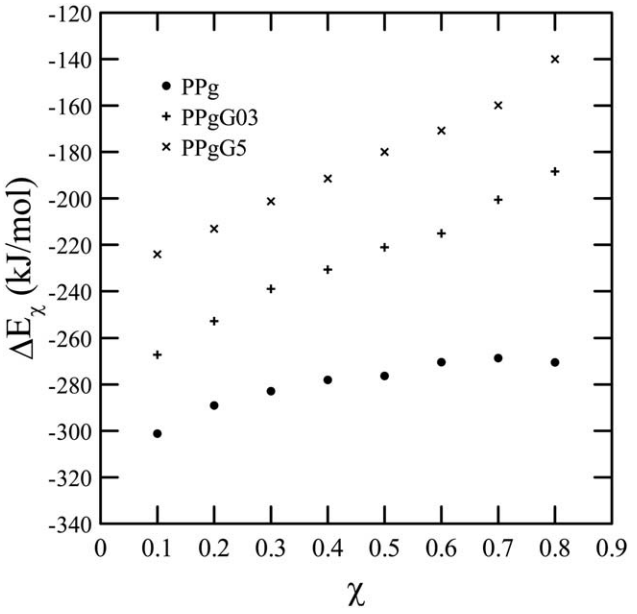

Figure 15. Activation energy of crystallization as a function of the crystallization enthalpy ratio, for PPg, PPgG03, and PPgG5.

suggest that nucleation is the controlling mechanism, while the change in trend that appears at higher χ is an evidence that the diffusion mechanism begins to affect the crystallization.[40] Additionally, it can be observed that in the modified polymers, $-\Delta E_\chi$ decreases linearly with χ, suggesting that nucleation is the controlling mechanism in PPgG03 and PPgG5, and that nucleation becomes easier as the temperature decreases (or the level of crystallization increases). Moreover, the value of $-\Delta E_\chi$ decreases with the concentration of glycerol for a given χ, implying that the crystallization is less restricted in the materials with LCBs.

Tian et al.[38] calculated values of $-\Delta E_\chi$ of 204 kJ mol^{-1} for a lineal PP and ~240 kJ mol^{-1} for three branched PPs at $\chi = 0.2$. Moreover, values of 217 and 180 were reported by Lonkar et al.[42] and Ardanuy et al.,[43] respectively, at the same χ. At this crystallization enthalpy ratio, PPg, PPgG03, and PPgG5 present values of $-\Delta E_\chi$ of 290, 250, and 210 kJ mol^{-1}, respectively. The larger value of the activation energy of PPg compared with that of PP agrees with the already mentioned effect of the anhydride groups that act as nucleating agents.[39] The modification of PPg reduces the amount of anhydrides and, consequently, the influence of this factor in the crystallization. Interestingly, the branched PPgGs have values of activation energies comparable to those of the branched PPs reported by Tian et al.,[38] suggesting that they have similar crystallization behavior.

CONCLUSIONS

Polypropylenes with LCBs were prepared by melt reaction of a maleic anhydride functionalized polypropylene and different concentrations of glycerol. The band that appears at about 1735 cm^{-1} in the FTIR spectra of the modified polymers indicate the formation of ester groups that confirm the reaction between the OH groups of glycerol and the anhydrides of PPg.

The chromatograms of the PPgGs display bimodal distributions of molecular weights and evidence of gel fraction is found with glycerol concentrations above 0.6 wt %. The modified materials present one peak corresponding to the remaining population of unmodified PPg, and a second peak placed at smaller retention volumes that correspond to new macromolecules of larger molecular weight. For glycerol concentrations up to 0.6 wt %, the former peak decreases gradually with the concentration of glycerol while that of the other peak gets larger. The analysis of the intrinsic viscosity data as a function of molecular weight, according to the model of Zimm and Stockmayer, reveals that the larger generated macromolecules present up to 4 branches every 10^4 carbons.

The formation of branched structures was confirmed by small-amplitude oscillatory shear experiments. Several rheological plots were used to investigate the linear viscoelastic properties of the PPgGs. As the concentration of glycerol increases, the dynamic properties become significantly enhanced in comparison with those of the original PPg, being the effect more noticeable in G' and mainly at low frequencies. This behavior implies the presence of a long relaxation time mode and agrees with the increasing complexity of the modified molecules. The highly modified materials even display gel-like behavior. The PPgGs also display thermorheological complexity and enhanced activation energy at low frequencies.

The analysis of the crystallization process shows that the anhydride groups in PPg and the LCBs have opposite nucleating effects since the former decreases and the later increases as the concentration of glycerol augment. Moreover, PPg presents the largest absolute value of activation energy of crystallization, which decreases with the concentration of glycerol for a given level of crystallization.

CREDIT FOR AUTHORSHIP

Jorge Guapacha was in charge of the acquisition of the data presented in this article and he participated in the analysis and interpretation of the results. The other authors, Marcelo Failla, Enrique Vallés and Lidia Quinzani, contributed to research design and to the analysis and interpretation of the data. All the authors were involved in writing the article and they give their approval to the submitted version.

ACKNOWLEDGMENTS

The authors are grateful for the financial support given by the National Research Council of Argentina (CONICET), the Universidad Nacional del Sur (UNS), the Agencia Nacional de Promoción Científica y Tecnológica (ANPCyT) and the CYTED Project 311RT0417.

REFERENCES

1. Moore, E. P., Jr. Polypropylene Handbook; Hanser: Munich, **1996**.
2. Gahleitner, M. *Prog. Polym. Sci.* **2001**, *26*, 895.
3. Han, C. D. Rheology and Processing of Polymeric Materials: Polymer Rheology; Oxford University Press: New York, **2007**; Vol. *1*.
4. Lu, B.; Chung, T. C. *Macromolecules* **1999**, *32*, 8678.

5. Rätzsch, M. *J. Macromol. Sci. A* **1999**, *36*, 1759.
6. Sugimoto, M.; Tanaka, T.; Masubuchi, Y.; Takimoto, J.; Koyama, K. *J. Appl. Polym. Sci.* **1999**, *73*, 1493.
7. Lagendijk, R. P.; Hogt, A. H.; Buijtenhuijs, A.; Gotsis, A. D. *Polymer* **2001**, *42*, 10035.
8. Rätzsch, M.; Arnold, M.; Borsig, E.; Ra, M.; Bucka, H.; Reichelt, N. *Prog. Polym. Sci.* **2002**, *27*, 1195.
9. Graebling, D. *Macromolecules* **2002**, *35*, 4602.
10. Auhl, D.; Stange, J.; Münstedt, H.; Krause, B.; Voigt, D.; Lederer, A.; Lappan, U.; Lunkwitz, K. *Macromolecules* **2004**, *37*, 9465.
11. Auhl, D.; Stadler, F. J.; Münstedt, H. *Macromolecules* **2012**, *45*, 2057.
12. Gotsis, D.; Zeevenhoven, B. L. F.; Hogt, H. *Polym. Eng. Sci.* **2004**, *44*, 973.
13. Paavola, S.; Saarinen, T.; Löfgren, B.; Pitkänen, P. *Polymer* **2004**, *45*, 2099.
14. Ye, Z.; Alobaidi, F.; Zhu, S. *Ind. Eng. Chem. Res.* **2004**, *43*, 2860.
15. Nam, G. J.; Yoo, J. H.; Lee, J. W. *J. Appl. Polym. Sci.* **2005**, *96*, 1793.
16. Krause, B.; Voigt, D.; Ha, L.; Auhl, D.; Mu, H. *J. Appl. Polym. Sci.* **2006**, *100*, 2770.
17. Tian, J.; Yu, W.; Zhou, C. *Polymer* **2006**, *47*, 7962.
18. Langston, J.; Colby, R. H.; Chung, T. C. M.; Shimizu, F.; Suzuki, T.; Aoki, M. *Macromolecules* **2007**, *40*, 2712.
19. Fina, A.; Tabuani, D.; Peijs, T.; Camino, G. *Polymer* **2009**, *50*, 218.
20. Li, S.; Xiao, M.; Wei, D.; Xiao, H.; Hu, F.; Zheng, A. *Polymer* **2009**, *50*, 6121.
21. Mabrouk, K. E.; Parent, J. S.; Chaudhary, B. I.; Cong, R. *Polymer* **2009**, *50*, 5390.
22. Su, F.-H.; Huang, H. *J. Appl. Polym. Sci.* **2009**, *113*, 2126.
23. Hingmann, R.; Marczinke, B. L. *J. Rheol.* **1994**, *38*, 573.
24. Bettini, S. H.; Agnelli, J. *Polym. Test.* **2000**, *19*, 3.
25. Arroyo, M.; Lopez-Machado, M. A.; Avalos, F. *Polymer* **1997**, *38*, 5587.
26. Silverstein, R. M.; Bassler, G. C.; Morrill, T. C. Spectrometric Identification of Organic Compounds, 5th ed.; Wiley: New York, **1991**.
27. Guapacha, J. *Synthesis and characterization of branched polypropylene by reactive mixing, PhD Thesis; Universidad Nacional del Sur*, **2014**.
28. Brandrup, J.; Immergut, E. H.; Grulke, E. A. Polymer Handbook, 4th ed.; Wiley: New York, **1999**.
29. Meijerink, N. L. J.; Schoffeleers, H. M.; Brands, A. M. G. *J. Appl. Polym. Sci.* **1984**, *29*, 3763.
30. Zimm, B. H.; Stockmayers, W. H. *J. Chem. Phys.* **1949**, *17*, 1301.
31. Zimm, B. H.; Kilb, R. W. *J. Polym. Sci.* **1959**, *37*, 19.
32. Lecacheux, D.; Lesec, J.; Quivoron, C. *J. Appl. Polym. Sci.* **1982**, *27*, 4867.
33. Berry, G. C. *J. Polym. Sci. Polym. Phys. Ed.* **1971**, *9*, 687.
34. Roovers, J.; Toporowski, P.; Martin, J. *Macromolecules* **1989**, *22*, 1897.
35. Wood-Adams, P.; Dealy, J. M.; deGroot, A. W.; Redwine, O. D. *Macromolecules* **2000**, *33*, 7489.
36. Wood-Adams, P.; Costeux, S. *Macromolecules* **2001**, *34*, 6281.
37. Keßner, U.; Münstedt, H. *Polymer* **2010**, *51*, 507.
38. Tian, J.; Yu, W.; Zhou, C. J. *J. Appl. Polym. Sci.* **2007**, *104*, 3592.
39. Seo, Y.; Kim, J.; Kim, K. U.; Kim, Y. C. *Polymer* **2000**, *41*, 2639.
40. Yang, B.; Yang, M.; Wang, W.; Zhu, S. *Polym. Eng. Sci.* **2012**, *52*, 21.
41. Vyazovkin, S. *Macromol. Rapid Commun.* **2002**, *23*, 771.
42. Lonkar, S. P.; Morlat-Therias, S.; Caperaa, N.; Leroux, F.; Gardette, J. L.; Singh, R. P. *Polymer* **2009**, *50*, 1505.
43. Ardanuy, M.; Velasco, J. I.; Realinho, V.; Arencón, D.; Martínez, A. B. *Thermochim. Acta* **2008**, *479*, 45.